Photocatalytic Layer-by-Layer Coatings for Degradation of Acutely Toxic Agents

Kevin C. Krogman, Nicole S. Zacharia, Doris M. Grillo, and Paula T. Hammond*

Department of Chemical Engineering, Massachusetts Institute of Technology, 77 Massachusetts Avenue, Cambridge, Massachusetts 02139

Received October 29, 2007. Revised Manuscript Received December 6, 2007

Highly reactive layer-by-layer (LbL) films have been developed as protective coatings intended for application on fibers worn by military personnel. In this work, the anionic species are titanium dioxide nanoparticles ranging from 5 to 10 nm in size, which are prepared in a stable colloidal solution specifically designed for this application, while the cationic species can be one of several traditional synthetic polycations, including weak and strong polyelectrolytes. The resulting coatings are mechanically stable and offer selective protection when the wearer is exposed to UV radiation (e.g.,sunlight); whereas the inherent water transmissive nature of the multilayers allows for much greater water vapor transport rates as compared to an inert rubber barrier material. Permeation tests of coated materials were conducted in a specially engineered cell by exposing the materials to a CWA simulant. In the extreme case, when a coated material is subjected to a saturated vapor of the CWA simulant, UV exposure resulted in a 95% decrease in toxic agent permeation. Furthermore, the coating can be deposited via a spray-LbL technique developed specifically for rapid, uniform deposition over large areas of textile materials at ambient temperatures and moderate pressures.

Introduction

Increasing concern over the use of chemical warfare, combined with more frequent potential exposure to toxic chemical environments faced by soldiers and emergency care providers, has heightened the need for new protective measures. Although traditional protective gear for toxic cleanup or exposure has relied on thick layers of dense rubber and/or activated charcoal liners, which act primarily as diffusive barriers to resist mass transfer, this strategy is not tenable for routine daily duty. Reactive coatings, which are able to selectively degrade toxic chemicals, including chemical warfare agents (CWAs) and environmental toxins such as NO_x and SO_x, whereas still affording the wearer a high degree of water vapor permeability and thus greater comfort, are an interesting strategy for protection against low to moderate level exposure. Such coatings could also provide a route to self-cleaning or decontaminating surfaces or fabrics for military or commercial use.

One means of eliminating airborne toxins that has received attention involves the photocatalytic degradation of toxic organic compounds using titanium dioxide[1–4] to generate superoxide anions, or mixed TiO_2/SiO_2 catalysts[5–7] to increase the material's bandgap and aid in volatile compound adsorption. Although these strategies exhibit excellent degradative capabilities, the technique of depositing unbound powders or nanoparticles on a surface does not form a sufficiently robust coating for application on personal protective equipment. Titania has also been introduced directly into fibers via electrospinning,[8] or into bulk films via traditional sol–gel routes.[9] Unfortunately, as the size of the titania entity increases, it becomes more difficult to introduce the particles into a mechanically stable polymer film. The work reported here presents a strategy to achieve the success demonstrated by prior titania based systems from an ultrathin, transmissive, and mechanically stable coating that can be readily deposited on traditional military clothing and packaging, as well as a variety of other substrates including electrospun materials. Such a coating can be tuned for its mechanical and chemical properties via the choice of polyamine and the incorporation of other polyelectrolytes so as to achieve the reactive protection described above, while existing in a form that is durable enough to withstand the rigors of daily activity and sufficiently discrete so as not to hinder the performance of the underlying material. We have developed a coating that can be readily deposited by the versatile layer-by-layer (LbL) deposition method[10] and provides a reactive barrier of more than 99% efficiency against a saturated environment of the

* Corresponding author. E-mail: hammond@mit.edu. Phone: (617) 258-7577. Fax: (617) 258-5766.

(1) Thompson, T. L.; Panayotov, D. A.; Yates, J. T.; Martyanov, I.; Klabunde, K. *J. Phys. Chem. B* **2004**, *108*, 17857.
(2) Martyanov, I.; Klabunde, K. *Environ. Sci. Technol.* **2003**, *37*, 3448.
(3) Vorontsov, A. V.; Lion, C.; Savinov, E.; Smirniotis, P. *j. Catalysis* **2003**, *220*, 414.
(4) Kleinhammes, A.; Wagner, G. W.; Kulkarni, H.; Jia, Y.; Zhang, Q.; Qin, L.; Wue, Y. *Chem. Phys. Lett.* **2005**, *411*, 81.
(5) Rodrigues, S.; Uma, S.; Martyanov, I.; Klabunde, K. *Abstracts of the 39th Midwest Regional Meeting of the American Chemical Society*, Manhattan, KS, Oct 20–22, 2004; American Chemical Society: Washington, D.C., 2004.
(6) Panayotov, D.; Kondratyuk, P.; Yates, J. T. *Langmuir* **2004**, *20*, 3674.
(7) Martyanov, I. N.; Klabunde, K. J. *J. Catal.* **2004**, *225*, 408.
(8) Madhugiri, S.; Sun, B.; Smirniotis, P.; Ferraris, J.; Balkus, K. *Microporous Mesoporous Mater.* **2004**, *69*, 77.
(9) Yusuf, M.; Imai, H.; Hirashima, H. *J. Sol−Gel Sci. Technol.* **2002**, *25*, 65.
(10) Decher, G. *Science* **1997**, *277*, 1232.

10.1021/cm703096w CCC: $40.75
Published on Web 02/07/2008

sulfur mustard simulant compound chloroethyl ethyl sulfide (CEES) when exposed to ultraviolet radiation. Although similar recent approaches have been taken to introduce titania nanosheets into photocatalytic LbL films,[11–13] the resulting coatings were shown to degrade organic hydrocarbons at relatively low quantities over time scales on the order of days; personal protective equipment, on the other hand, must have degradative properties on the time scale of minutes, at most, to be of any practical use. Furthermore, there is general concern that titania containing coatings suffer decreased chemical stability on exposure to UV. However, we have found the systems reported here to remain intact even after high-yield conversions of simulant agent.

The process of LbL film deposition involves the sequential exposure of a charged substrate to an alternating series of solutions of oppositely charged species. Upon exposure to each solution the effective charge exhibited by the surface is reversed, through adsorption of charged species, before proceeding to the next solution. The cycle can be repeated any desired number of times to develop a highly uniform coating of precisely controllable thickness on the substrate. This method typically employs polyelectrolytes adsorbed from dilute aqueous solutions; however, charged colloidal species can also be incorporated into the films.[14,15] In some instances, charged rigid nanoparticles can take the place of one[16] or even both[17] of the charged polyelectrolytes. It is in this manner that we have been able to incorporate reactive titanium dioxide nanoparticles of very small diameter, and therefore large reactive surface area, into a mechanically cohesive film coating. In our approach an automated spraying method is used,[18–20] allowing us to rapidly coat a variety of complex substrate geometries and materials including, but not limited to, cotton textile and protective plastic film.

Experimental Section

LbL Solutions. Poly(dimethyldiallylammonium chloride) (PDAC, MW = 100 000), and sodium chloride were purchased from Aldrich and used to make a solution of 20 mM concentration with respect to the repeat unit of PDAC, and 10 mM with respect to NaCl, in DI water. Colloidal titania nanoparticles were synthesized by slowly combining a solution of 1 part tetrabutyl ammonium hydroxide and 50 parts absolute ethanol with a solution of 1 part titanium (IV) isopropoxide and 6 parts absolute ethanol by volume as shown in Scheme 1. The combined solution was then slowly diluted with DI water to 4 times its original volume under rapid stirring, and refluxed for 3 days at 100 °C. All chemicals were used as purchased from Aldrich. The resulting colloidal solution was analyzed using a Brookhaven Instruments Corp. ZetaPALS Zeta-potential analyzer and, upon evaporation, a Rigaku Powder X-ray Diffractometer.

Scheme 1. (a) Reaction Scheme by Which Colloidal Titania Solution Is Created;[a] (b) Charged Species Deposited Alternately in Film Construction

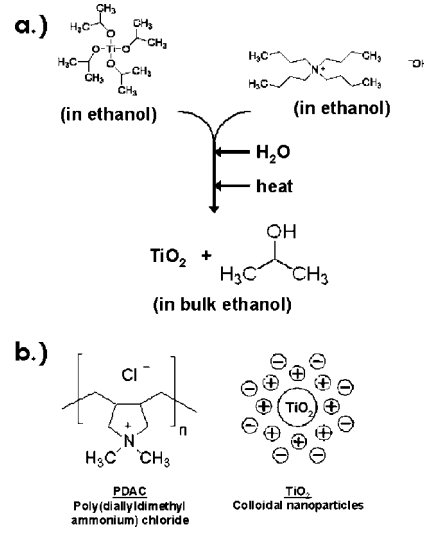

[a] Upon generation of the stabilized nanoparticles in a solvent mixture of water, ethanol, and isopropanol, the alcohols can safely be removed by continued heating resulting in a stable aqueous solution of colloidal particles.

Coating Deposition and Analysis. LbL deposition was conducted on Saran 8 plastic sheeting (12.7 μm thickness) used as purchased from Dow Chemical. Prior to deposition the plastic sheeting was rinsed with methanol and exposed to an oxygen plasma (Harrick PCD 32G) for 5 min to clean and hydroxylate the surface. Both solutions as well as rinsewater were titrated to pH 10 using HCl. Deposition was conducted using an automated spray-LbL system.[18] All solutions were delivered by ultrahigh purity Argon gas regulated to 50 psi. PDAC was sprayed for 3 s and allowed to drain for 17 s, before spraying with water for 10 s and allowing it to drain for 10 s. The half-cycle was repeated for the colloidal titania solution resulting in an 80 s cycle, whereas the full cycle was repeated 50 times to create the final coating tested here. Film thickness was determined on a Woolam XLS-100 spectroscopic ellipsometer and checked using a Tencor P10 Profilometer, whereas titania composition was determined using a TA Instruments TGAQ50 thermogravimetric analyzer.

Permeation Testing. Permeation testing was conducted in a stainless steel cell using ultrapure compressed air for the sweep gas. The contaminated stream was analyzed using a Gow-MAC Instrument Co. Series 23–550 total hydrocarbon analyzer equipped with a flame ionization detector. The detector was calibrated for CEES using a certified working class calibration standard 100 ppm mixture of chloroethyl ethyl sulfide in nitrogen (Scottgas). UV illumination was provided by a Blue Wave 200 (Dymax) UV spot source filtered to ~100 mW/cm^2. Samples were challenged using chloroethyl ethyl sulfide (CEES) available from Aldrich. CEES is a vesicant compound which can cause blisters if it comes in contact with the skin. Although it is a less toxic simulant for mustard gas, extreme caution should be exercised particularly when working with CEES vapors. FTIR testing was conducted using a Nexus 870 FTIR ESP (Thermo Nicolet) in a quartz gas cell with a 10 cm path length.

Film Construction. We begin by synthesizing titanium dioxide nanoparticles via a controlled hydrolysis utilizing a modified sol–gel process. By limiting the rate at which the hydrolysis reaction converts titanium(IV) isopropoxide into titanium dioxide, we are

(11) Sasaki, T.; Ebina, Y.; Watanabe, M.; Decher, G. *Chem. Commun.* **2000**, 2163.
(12) Sasaki, T.; Ebina, Y.; Fukuda, K.; Tanaka, T.; Harada, M.; Watanabe, M. *Chem. Mater.* **2002**, *14*, 3524.
(13) Shibata, T.; Sakai, N.; Fukuda, K.; Ebina, Y.; Sasaki, T. *Phys. Chem. Chem. Phys.* **2007**, *9*, 2413.
(14) Iler, R. K. *J. Colloid Interface Sci.* **1966**, *21*, 569–594.
(15) Lvov, Y.; Ariga, K.; Onda, M.; Ichinose, I.; Kunitake, T. *Langmuir,* **1997**, *13*, 6195.
(16) Kotov, N. A.; Dekany, I.; Fendler, J. H. *J. Phys. Chem.* **1995**, *99*, 13069.
(17) Lee, D.; Rubner, M. F.; Cohen, R. E. *Nano Lett.* **2006**, *6*, 2305.
(18) Krogman, K. C.; Zacharia, N. S.; Schroeder, S.; Hammond, P. T. *Langmuir* **2007**, *23*, 3137.
(19) Schlenoff, J. B.; Dubas, T.; Farhat, T. *Langmuir* **2000**, *16*, 9968.
(20) Izquierdo, A.; Ono, S. S.; Voegel, J.-C.; Schaaf, P.; Decher, G. *Langmuir* **2005**, *21*, 7558.

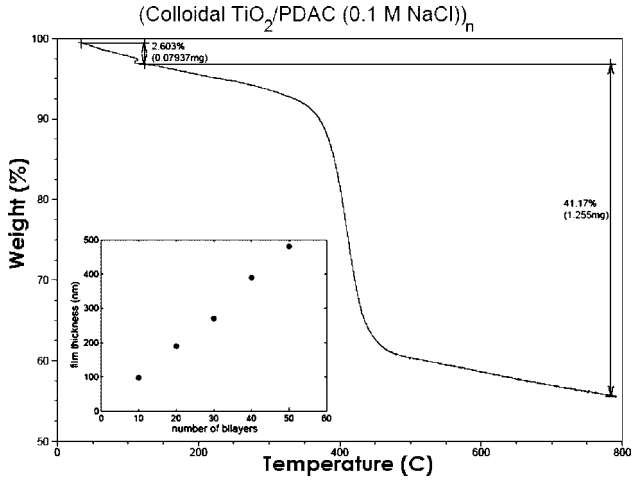

Figure 1. Characterization of as deposited (colloidal TiO_2/PDAC)$_n$ films. Depositing all solutions at pH 10 results in a film that is ~56% TiO_2 at ambient conditions as determined by thermogravimetric analysis. This film is deposited at a linear rate of ~10 nm per bilayer (inset). Reported thicknesses are averages taken from several data points on a silicon wafer and vary by less than ±10 nm across the matrix.

able to create a monodisperse colloidal suspension of titanium dioxide nanoparticles exhibiting 5–10 nm diameters. Further investigation with X-ray diffraction indicates that the particles are of the anatase phase, which is preferred for the nanoparticles to act as a photocatalyst. Zeta-potential analysis by phase analysis light scattering (Zeta-PALS) indicates that the particles carry a mean surface charge of roughly −34 mV, implying the solution conditions are far enough removed from the isoelectric point of the amphoteric titania to ensure that the suspended particles are more than sufficiently charged to participate in LbL deposition.

A photocatalytic coating can then be deposited by alternating adsorption between the synthesized colloidal solution and a solution of a polycationic material, which in this case is poly(dimethyldiallylammonium chloride), chosen for its strong polyelectrolyte properties and thus the independence of its degree of ionization with respect to solution pH. Because a spray-LbL system is utilized,[18–20] the coatings are developed at the rate of one "bilayer" cycle every 80 s, allowing for the creation of a 50 bilayer film in slightly more than one hour of process time.

Results and Discussion

Multilayer coatings were generated via the alternating misting of a 10 wt % solution of titanium dioxide nanoparticles and a 20 mM solution of PDAC. All solutions, including rinsewater, were titrated to pH 10 prior to deposition. As shown in Figure 1, the growth of the (TiO_2/PDAC)$_n$ films proceeds linearly at a constant rate of approximately 10 nm per deposition cycle, suggesting that TiO_2 particles are adsorbed to the developing surface as a monolayer during each exposure to colloidal solution. An example thermogravimetric analysis (TGA) performed on one such film constructed under these conditions can also be seen in Figure 1. Starting at ambient conditions, we find that approximately 2.6% of the film's weight at equilibrium is water, whereas 41% of the film is combustible organic material. Upon heating to 800 °C and holding for several hours, it is observed that titania comprises approximately 56% of the film by weight.

The resulting film is mechanically stable, as a result of the strong electrostatic interactions between the charged

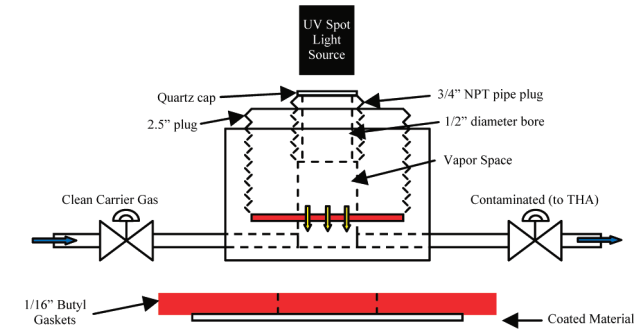

Figure 2. Permeation cell in which photocatalytic testing was conducted. The cell design restricts mass transfer to one dimension through the coated material (represented by yellow arrows), whereas the entire surface area through which permeant is passing can be uniformly exposed to ultraviolet radiation.

Scheme 2. Testing Method by Which Spray-LbL Deposited Coatings Are Tested for Photocatalytic Degradation of Volatile Organic Compounds

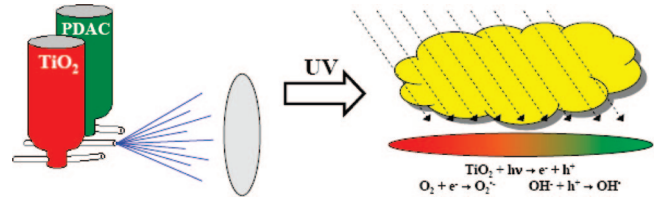

Coatings are deposited, dried, and mounted in a sealed test chamber where they are exposed to the VOC and UV radiation.

species. Hence, even though it is comprised of 56 wt % rigid nanoparticles, it is able to resist gentle rubbing. This result can be attributed to the strong charge observed on the surface of the synthesized colloidal nanoparticles, as well as the intermolecular entanglements of the codeposited polyion.

Permeation Testing. To conduct the desired reactive mass transfer tests a stainless steel permeation cell, represented schematically in Figure 2, was specifically designed and engineered. A coated substrate sample is sandwiched, along with a 1/16 in. butyl rubber gasket of the same outer diameter as the sample and 13/16 in. inner diameter, between the face of a stainless steel plug and the base of the cell. The plug has been bored through to accommodate a second smaller plug, which then encloses a vapor space of known volume above the coated sample. It is into this vapor space that a specific dose of condensed phase CEES is introduced as shown in Scheme 2. As simulant vaporizes from the condensed source, the concentration of CEES in the vapor space is maintained at its saturation vapor pressure ($C_{sat} \approx$ 5000 ppm) for an extended period of time until the source is consumed and the test is complete. The smaller plug is capped with a quartz wafer providing negligible adsorption of radiation in the ultraviolet wavelengths down to 200 nm. One face of the sample material is exposed to a known concentration of CEES vapor, whereas below the sample, a stream of ultrapure carrier gas is passed at a flow rate that is sufficiently large to ensure the partial pressure of simulant on the permeant side of the sample is negligibly small. Thus a known cross-sectional area of the sample is exposed to a saturated environment of CWA simulant creating a driving force for mass transfer in the form of a concentration

gradient. The exposed cross-sectional diameter has been chosen so as to eliminate edge diffusion effects (i.e., sample thickness ≪ cross-sectional diameter) simplifying the analysis by causing mass transfer to be predominantly unidirectional.

Vaporized CEES from the vapor space dissolves into the LbL coating of the sample which may or may not be photocatalytically active during the test. CEES, or the appropriate products of degradation, then diffuse through the inert substrate before leaving the sample into the carrier gas on the permeant side of the substrate. The carrier gas is then analyzed by combustion in the hydrogen/oxygen flame of a total hydrocarbon analyzer equipped with an FID capable of contaminant detection at 0.01 ppm levels. Similarly, the test can also be run in conjunction with an ultraviolet spot source, equipped with a mercury vapor lamp to mimic sunlight. The lamp is capable of illuminating the exposed portion of the sample through the quartz cap above the vapor space, eliminating the risk of contamination between the UV lamp and the vapor space.

The mass flux of contaminant through the sample can then be determined by measuring the concentration of contaminant in the sweep gas, as well as the flow rate at which the sweep gas is passing under the sample. Similarly, the rate at which contaminant passes through the sample can be normalized by the cross-sectional area through which mass transfer is allowed to occur, specified by the cell geometry, and the driving force for mass transfer in the form of a partial pressure gradient. Termed the permeance, the normalized flux can be calculated, $P = q/A\Delta p = f(F_{\text{carrier}}, ppm_{\text{CEES}})$, by measuring the flow rate of carrier gas as well as the concentration of CEES contaminant in the stream. The calculation gives a thickness independent interpretation of the exposure a user would expect to experience while under the protection of such a coated substrate.

Photocatalytic Capabilities. For the purpose of testing the photocatalytic capabilities of the $(PDAC/TiO_2)_n$, a 50-cycle deposition was performed using the spray-LbL technique. The film was constructed on a 12.7 μm thick nonporous poly(vinylidene chloride) sheet available under the trade name Saran 8 from the Dow Chemical Company. This substrate material was chosen for several reasons. The inherent negative surface charge on the plastic sheet enables the adherence of the first few monolayers to the substrate via electrostatic interactions. Further, by choosing a nonporous substrate with easily characterizable gas permeation properties, it is possible to determine mass-transfer characteristics of the uncoated substrate to serve as a benchmark for future comparisons with the coated material. Saran is a biaxially oriented monolayer barrier film which is moderately CEES permeable, a property that is quantified below. It is also inert to chlorinated compounds such as CEES, making it an ideal substrate for permeation testing of $(PDAC/TiO_2)_n$ reactive coatings.

The coated sample was then mounted in the permeation cell, and 3 μL of condensed phase CEES were introduced into the vapor space above the sample. As the vapor permeated through the sample it was collected and swept away to the Total Hydrocarbon Analyzer (THA) which was calibrated for CEES identification. The resulting mass flux, in grams of CEES per minute, can be seen in Figure 3. During the first 15 min of testing no contaminant is observed in the permeant vapor. After this breakthrough time, $t_{b,dark}$, however, the concentration of CEES in the sweep gas continues to increase as the sample becomes loaded with CEES. The parabolic downturn occurs as the condensed source of CEES in the vapor space becomes depleted and is no longer able to maintain a constant vapor pressure above the sample. A maximum concentration of CEES in the permeant stream is observed at 33 ppm. The test is conducted for 2 h, which is sufficient for the large majority of the CEES to exit the system.

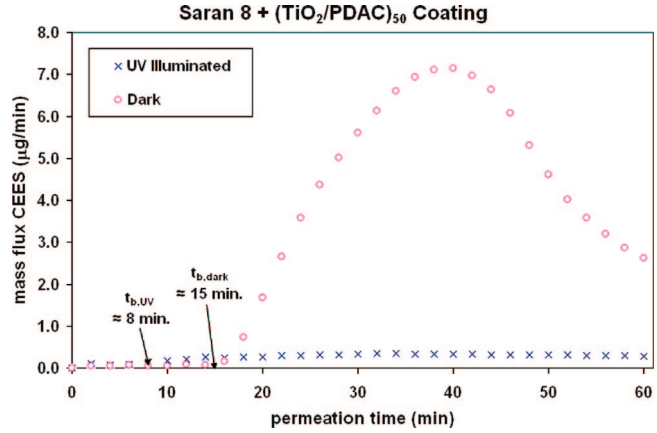

Figure 3. Mass flux of CEES through a coated sample as measured in the carrier gas passing below the sample. Identical samples were exposed to 3 μL loadings of CEES and allowed to permeate. The test was conducted both with (X) and without (O) UV illumination.

Upon complete evacuation of CEES from the system, further testing can be conducted. An identical film was subjected to a similar 3 μL loading. This time, however, ultraviolet light was passed through the quartz cap of the cell, illuminating the area of the coated sample simultaneously exposed to the saturated atmosphere of CEES. Again, permeant vapor is removed by the sweep gas and analyzed by the THA. The observed instantaneous mass flux can also be seen in Figure 3. In this scenario, no contaminant is detected by the THA prior to a shorter 8 min breakthrough time, $t_{b,UV}$. This can be explained by the solution-diffusion mechanism by which CEES transfers across the material. Permeability is typically expressed as the product of the diffusivity of a molecule through the solid matrix and the solubility of the vapor molecule in the solid.[21] As the intense UV radiation falls on the titania particles some of the energy is used to generate electron–hole pairs that eventually result in the superoxide anions that make titania useful as a photocatalyst. The remainder of the energy is absorbed as radiant heat, slightly increasing the temperature of the underlying solid material. This rise in temperature will serve to increase both the diffusivity and the solubility of CEES throughout the sample. A slight increase in permeation rate is thus not surprising, and the contaminant molecules appear twice as rapidly in the permeant stream.

Aside from the temperature-induced decrease in resistance to mass transfer, it is clear that the overall CEES permeation

(21) Wijmans, J. G.; Baker, R. W. *J. Membr. Sci.* **1995**, *107*, 1.

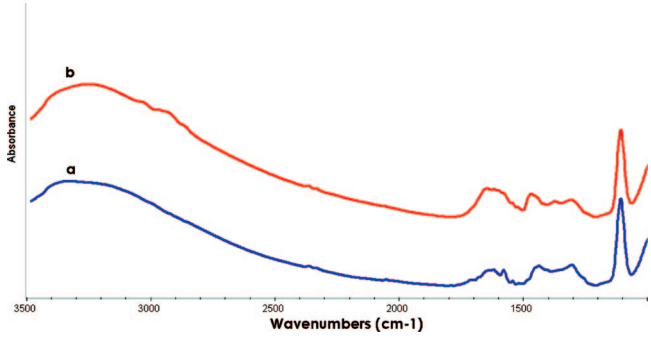

Figure 4. FTIR spectra of (a) the as-deposited (colloidal TiO_2/PDAC)$_{50}$ coating on IR transparent silicon, and (b) the same coating after 60 min of UV exposure.

has been greatly reduced. This effect becomes even more pronounced as time passes. The peak concentration of CEES in the permeant vapor occurs at roughly the same elapsed time, but the degradation of CEES vapor in the photocatalytic coating has reduced this peak value to less than 1.5 ppm. Thus the reduction in maximum CEES concentration on the permeant side of the sample membrane was decreased by more than 95% when subjected to UV light. It is also beneficial to analyze the protective capabilities of the film from a net exposure standpoint. Because these tests have been conducted with 3 μL loadings of CEES, a stoichiometric constraint imposed by the amount of oxygen present in the vapor space available to participate in the photocatalytic reaction at the titania surface, this type of analysis is only appropriate up to the point where the condensed CEES source appears to run out. After this time, the vapor space is no longer maintained at the saturation concentration as CEES is reactively consumed by the film, and the partial pressure gradient driving mass transfer begins to decrease. This appears to occur at approximately 40 min of test time. Up to this point, only 5.1 μg of CEES have passed through the photocatalytically active (i.e., exposed to UV light) sample. This corresponds to less than 1% of the 3.21 mg of CEES introduced into the vapor space. A more thorough understanding of the net flux over longer periods of time is necessary to fully evaluate this material and will be obtained in the future after some modifications to the test cell. However, it can be concluded from these preliminary results that the (colloidal TiO_2/PDAC)$_{50}$ coating, when illuminated by UV light, can exhibit reactive protection for at least 40 min of more than 99% from a saturated environment of CEES.

The net mass flux over the 1 h time frame displayed in Figure 3 can also be calculated by integrating the instantaneous flux over the length of the test. In the dark membrane test, this net flux corresponds to 104 μg, while the UV illuminated test results in 8.2 μg net permeation. By forming a ratio of the net flux observed in the presence of UV light to that observed without UV light, a 10-fold reduction is seen. This 10-fold reduction can then be expected in further testing independent of the fact that a steady state scenario was never actually reached in these tests. As mentioned above, a benefit of using a nonporous substrate such as Saran 8 is that material mass transfer properties can be determined using this type of permeation cell by simply increasing the

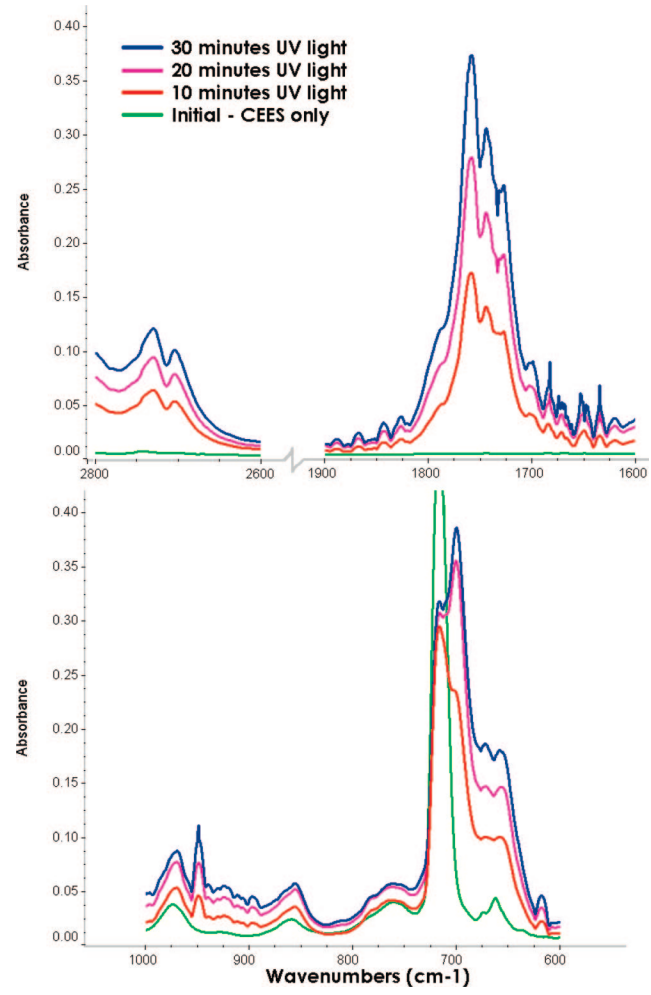

Figure 5. FTIR spectra collected during a closed cell batch analysis. The cell contained a sample of coated material, equal in size to the exposed surface during permeation testing, and 3 μL condensed CEES. The entire cell was then irradiated by UV light and spectra taken at 10 min time intervals.

condensed CEES loading until a steady state diffusion scenario is obtained. The increased loading provides a larger condensed phase source capable of maintaining the saturated vapor space until the sample reaches diffusional equilibrium. Prior to these tests it was determined that the steady-state concentration of CEES observed in the sweep gas, of identical flow rate, below a sample of uncoated Saran 8 was 152 ppm. This uncoated control test corresponds to a steady state mass flux of CEES through Saran 8 of 32.7 μg/min, five times greater than the largest rates observed in either of these tests. We can thus assume that the multilayer coating provides a significant portion of the resistance to mass transfer across the sample.

It has been suggested by previous work that ultraviolet illumination of LbL constructed films composed of titania nanosheets and PDAC will elicit the photocatalytic decomposition of the PDAC in the film, producing inorganic multilayers composed only of the titania nanosheets and charge balancing ammonium ions.[12] The resulting coating would presumably have a marked decrease in mechanical stability, as well as a change in film permeability over time as the structure collapses and the titania sheets are freed of the PDAC. If this were the case the formation of NH_4^+ upon

UV illumination, generated from the decomposition of PDAC, would be readily observable in the film via FTIR analysis as a sharp peak around 1427 cm^{-1} as well as three broad peaks in the 2800–3300 cm^{-1} range. As can be seen in Figure 4, UV exposure of the (colloidal TiO_2/PDAC)$_{50}$-coating for 60 min does not appear to generate these results. Although the sharp peak at 1107 cm^{-1} is clearly visible, because of Si−O−Si stretching from surface oxides on the silicon wafer, no peaks have been generated at 1427 cm^{-1}. Three very small peaks at 2861, 2934, and 3029 cm^{-1} can be seen, indicating that a small portion of the available PDAC has been photocatalytically decomposed, but this does not appear to have had an effect on the mechanical stability of the coating. Furthermore, it has recently been demonstrated that NO_3^- ions are a reasonable degradation product of short-chain alkyl amines as well.[22] However, no increase in absorption in the 1410–1340 cm^{-1} region is observed upon UV exposure. Even after intense UV exposure for 60 min the film still resists rubbing indicating that it has not undergone collapse of the interpartical galleries as a result of PDAC decomposition.

Photocatalytic Confirmation. It should be noted in Figure 3 that the tail of the data collected from the "dark" test extends for prolonged times at low values, as ever decreasing amounts of CEES desorb from the once-saturated film, and diffuse into the sweep gas over several hours. As less CEES is dissolved in the sample, the driving force to leave the solid and enter the gas stream decreases, and the appearance of several parts per million CEES for some time is to be expected. Rather than attempting to quantify the amount of CEES accounted for in these tails, we have chosen to focus the previous discussion on the peak dosage allowed during the early portions of the test. Thus, to confirm the presence of a photocatalytic degradation reaction and not simply a strong absorption of CEES with slow desorption over extended time periods, further testing was conducted on the UV-illuminated sample. A batch FTIR test was constructed by mounting a 0.51 $in.^2$ swatch (i.e., identical to the exposed cross-sectional area within the permeation cell) of coated sample in a sealed quartz gas cell. Again, 3 μL of condensed CEES were introduced into the cell through a septum and allowed to vaporize for 10 min, simulating the breakthrough period afforded by the sample in the permeation cell. The sample was then illuminated by the same UV source, and the vapor in the cell analyzed at ten minute intervals over a thirty minute test period. The simplified mechanism by which superoxide anions ($O_2^{\bullet -}$) and surface hydroxyl radicals ($OH^{\bullet}$) are generated and CEES is subsequently decomposed is as follows

$$TiO_2 + h\nu \rightarrow e^- + h^+ \quad (1)$$

$$O_2 + e^- \rightarrow O_2^{\bullet -} \quad (2a)$$

$$H_2O \rightarrow H^+ + OH^- \Rightarrow OH^- + h^+ \rightarrow OH^{\bullet} \quad (2b)$$

$$CEES + 7.5O_2^{\bullet -} \rightarrow 4CO_2 + 3H_2O + H_2SO_4 + HCl \quad (3)$$

The gas phase decomposition has been investigated and it has been shown that there are a variety of less toxic intermediate byproducts which are also observed.[2,3] When a photocatalytic reaction is occurring, the appearance of compounds such as ethylene, chloroethylene, acetaldehyde, chloroacetaldehyde, and carbon dioxide should be readily observable in the resulting vapor. Portions of the FTIR spectra taken initially and after 10, 20, and 30 min of UV irradiation can be seen in Figure 5.

Two broad peaks are observed in the 2750–2700 cm^{-1} range, while a strong triplet centered around 1750 ± 50 wavenumbers is observed to increase as the test proceeds. These suggest the presence of the carbonyl stretching band of acetaldehyde as well as chloroacetaldehyde.[23,24] Neither of these regions exhibit any IR absorption in gaseous CEES. A sharp peak appears at 950 cm^{-1} which is also clearly not present in the initial spectra containing only gaseous CEES. This band is present in an IR-fingerprint of ethylene as the ν_7 band, but may also be a result of chloroethylene present in the vapor.[25] The increase in absorbance at 668 cm^{-1} is indicative of the ν_2 band of carbon dioxide,[26] suggesting the increasing presence of one of the final products throughout the duration of the test. The conclusion can then be drawn that even in a saturated atmosphere the surface of the titania remains active for at least 30 min. A weak signal of several peaks is also observed at wavenumbers slightly less than 3000 cm^{-1}, similar to those recorded in previous photocatalytic degradation studies,[2] suggesting some HCl to be present in the gas phase. The relative weakness of this signal is not of concern, however, as most of the hydrogen chloride and sulfuric acid generated by the reaction is expected to remain bound to the titania surface. Typically these products can be responsible for the fouling and eventual elimination of the catalytically active sites on the titania surface; however, the observed steady increase of several byproducts in the gas phase indicate this has not succeeded in stifling the reaction over the course of this test.

Conclusion

These results present a unique way to synthesize and introduce titanium dioxide nanoparticles into a mechanically stable coating capable of the photocatalytic degradation of the chemical warfare agent simulant chloroethyl ethyl sulfide. The entire coating process, from synthesis to deposition, can be conducted at ambient temperatures and moderate pressures, and does not require expensive specialized equipment to produce. The process is readily scalable and can be conducted on substrates of limitless dimension and geometry based on the spray-LbL method by which the coating is applied. Sample coated plastics have been shown to provide more than 99% protection from a saturated atmosphere of

(22) Klare, M.; Scheen, J.; Vogelsang, K.; Jacobs, H.; Broekaert, J. A. C. *Chemosphere* **2000**, *41*, 353.
(23) Benvenutti, E. V.; Gusjikem, Y. *J. Braz. Chem. Soc.* **1998**, *9*, 469.
(24) VPL Molecular Spectroscopic Database. http://vpl.ipac.caltech.edu/spectra/frontpage.htm (2007).
(25) Baldwin, K. G. H.; Watts, R. O. *J. Chem. Phys.* **1987**, *87*, 873.
(26) Evans, C. S.; Hunneman, R.; Seeley, J. S.; Whatley, A. *Appl. Opt.* **1976**, *15*, 2736.

simulant when subjected to ultraviolet radiation with a spectrum resembling that of sunlight. Similarly, the polar ionic complex nature of LbL films allows the material to have much greater water vapor transport properties when compared to inert rubbers capable of similar protective properties. The coating is optically clear and can be deposited on materials without compromising their underlying functionality. Finally, because the titania is deposited as part of an exterior coating there is less risk that superoxide anions developed even under intense UV light will degrade the underlying material. While small portions of the polycation in the film are degraded by the photocatalytic activity of the titania, the mechanical stability of the coating is not compromised.

This research was supported in part by the U.S. Army through the Institute for Soldier Nanotechnologies under contract DAAD-19–02-D-0002 with the U.S. Army Research Office. The content does not necessarily reflect the position of the government, and no official endorsement should be inferred.

CM703096W